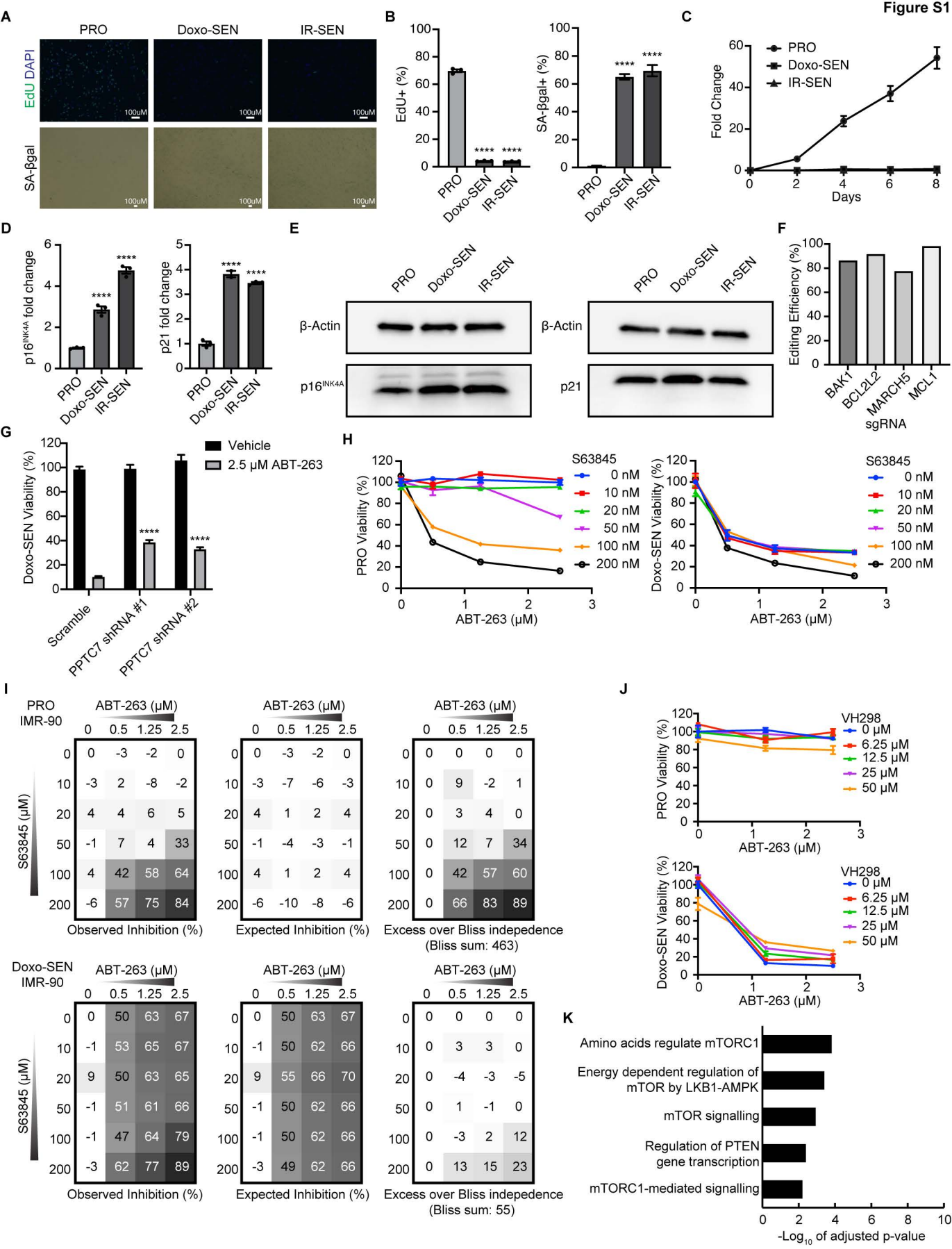
A
PRO
Doxo-SEN
IR-SEN
EdU DAPI
SA-βgal
100uM
B
EdU+ (%)
SA-βgal+ (%)
****
C
Fold Change
Days
PRO
Doxo-SEN
IR-SEN
D
p16INK4A fold change
p21 fold change
E
β-Actin
p16INK4A
p21
F
Editing Efficiency (%)
BAK1
BCL2L2
MARCH5
MCL1
sgRNA
G
Doxo-SEN Viability (%)
Vehicle
2.5 μM ABT-263
Scramble
PPTC7 shRNA #1
PPTC7 shRNA #2
H
PRO Viability (%)
Doxo-SEN Viability (%)
ABT-263 (μM)
S63845
0 nM
10 nM
20 nM
50 nM
100 nM
200 nM
I
PRO IMR-90
Doxo-SEN IMR-90
ABT-263 (μM)
S63845 (μM)
Observed Inhibition (%)
Expected Inhibition (%)
Excess over Bliss indepedence
(Bliss sum: 463)
(Bliss sum: 55)
J
VH298
0 μM
6.25 μM
12.5 μM
25 μM
50 μM
PRO Viability (%)
Doxo-SEN Viability (%)
ABT-263 (μM)
K
Amino acids regulate mTORC1
Energy dependent regulation of mTOR by LKB1-AMPK
mTOR signalling
Regulation of PTEN gene transcription
mTORC1-mediated signalling
-Log10 of adjusted p-value

Figure S1. Validations and summaries of Death-seq CRISPR senescence ABT-263 screen, related to Figure 1

(A) Representative images of EdU incorporation and SA-βgal 8 d after senescence induction in the proliferative (left), Doxo-induced senescent (middle), and Irradiation-induced senescent (right) IMR-90s. (B) Quantification of (A). (C) Growth curve of proliferative, Doxo-induced senescent, and Irradiation-induced senescent IMR-90s, starting 7 days after senescence induction. (D) mRNA expression of *p16*^{INK4a} and *p21* in IMR-90s were quantified by qRT-PCR and normalized by Tbp levels. (E) Western blot of p16^{INK4a} and p21 in IMR-90s. Loading control, β-Actin. (F) Confirmation of CRISPR sgRNA knockout editing efficiency in selected hit cell lines by TIDE analysis. (G) Validation of the genome-wide screen ABT-263 modifier hit, PPTC7, which inhibited cell death using individual-well shRNA knockdown compared to control shRNA. Cell viability was assessed after treatment with 2.5 μM ABT-263 for 3 d in Doxo-induced senescent IMR-90s. (H) Proliferative (PRO) (left) and Doxo-induced senescent IMR-90s (right) were treated with ABT-263 and the MCL1 inhibitor S63845 at the indicated concentrations for 3 d before viability was assessed relative to no drug control. (I) The percent expected inhibition is subtracted from the percent observed inhibition at each combination of drug doses in proliferative (top), and Doxo-induced senescent (bottom) IMR-90s to calculate drug synergy represented by excess over Bliss independence. (J) Proliferative (top) and Doxo-induced senescent (bottom) IMR-90s were treated with ABT-263 and the VHL inhibitor VH298 at the indicated concentrations for 3 d before viability was assessed relative to no drug control. (K) The top non-apoptosis related Reactome categories enriched in the 64 genes that passed 30% FDR in the genome-wide ABT-263 screen. Data are representative of two independent experiments performed in triplicate and presented as mean ± s.e.m. in panels (G-J). One-way ANOVA with Dunnett's post-hoc test, *P < 0.05, **P < 0.01, ***P < 0.001, ****P < 0.0001.

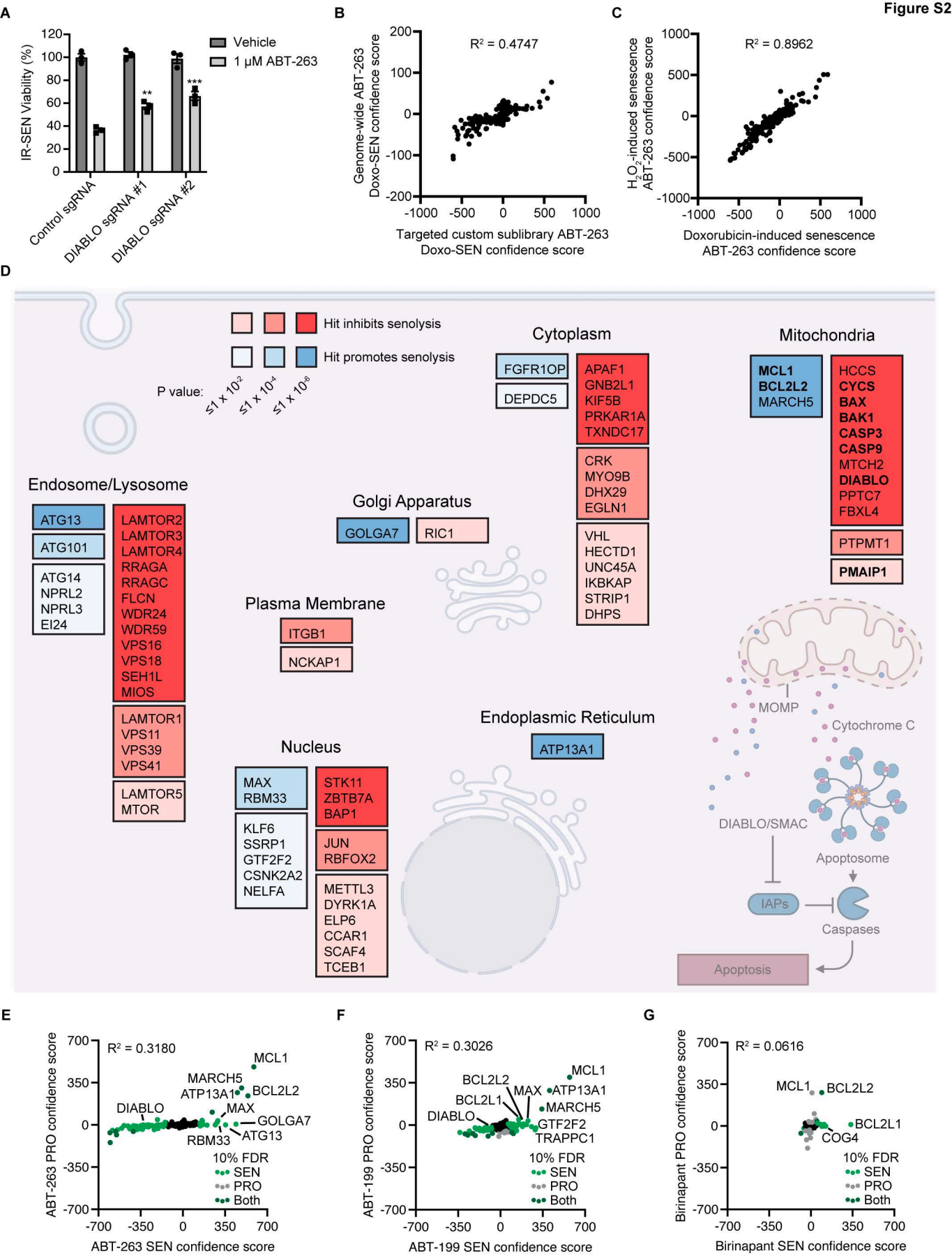
A
IR-SEN Viability (%)
Vehicle
1 μM ABT-263
Control sgRNA
DIABLO sgRNA #1
DIABLO sgRNA #2
B
R² = 0.4747
Genome-wide ABT-263 Doxo-SEN confidence score
Targeted custom sublibrary ABT-263 Doxo-SEN confidence score
C
R² = 0.8962
H2O2-induced senescence ABT-263 confidence score
Doxorubicin-induced senescence ABT-263 confidence score
D
Hit inhibits senolysis
Hit promotes senolysis
P value:
Cytoplasm
Mitochondria
Endosome/Lysosome
Golgi Apparatus
Plasma Membrane
Endoplasmic Reticulum
Nucleus
MOMP
Cytochrome C
DIABLO/SMAC
Apoptosome
IAPs
Caspases
Apoptosis
E
R² = 0.3180
ABT-263 PRO confidence score
ABT-263 SEN confidence score
10% FDR
SEN
PRO
Both
F
R² = 0.3026
ABT-199 PRO confidence score
ABT-199 SEN confidence score
G
R² = 0.0616
Birinapant PRO confidence score
Birinapant SEN confidence score

Figure S2. Targeted sublibrary senolytic Death-seq screens highlight importance of SMAC and systematically identify apoptosis pathway members, related to Figure 3
(A) Validation of DIABLO/SMAC sgRNA knockouts compared to control sgRNA cell viability after treatment with vehicle or 1 μM ABT-263 for 3 d in IR-induced senescent IMR-90s. (B) Correlation of combo casTLE confidence scores of the targeted custom sublibrary ABT-263 screen and genome-wide screen for all genes in the targeted custom sublibrary. R-squared value is from a linear regression model. (C) Correlation of combo casTLE confidence scores of the targeted custom sublibrary Doxo-induced senescence ABT-263 screen and the targeted custom sublibrary H_2O_2-induced senescence ABT-263 screen for all genes in the targeted custom sublibrary. R-squared value is from a linear regression model. Data are representative of two independent experiments performed in triplicate and presented as mean ± s.e.m. in panel (A). One-way ANOVA with Dunnett's post-hoc test, *P < 0.05, **P < 0.01, ***P < 0.001, ****P < 0.0001. (D) Schematic of the proteins encoded by hits which passed 10% FDR from the Doxo-SEN custom sublibrary ABT-263 screen with subcellular localizations according to UniProtKB and MitoCarta3.0. In bold are hits that are members of the MitoCarta3.0 apoptosis MitoPathway. Hits are color coded by significance (casTLE P values). (E-G) Correlation of combo casTLE confidence scores of the 1 μM ABT-263 24 h screen (E), 10 μM ABT-199 24 h screen (F), and 2 μM Birinapant 24 h screens (G) in Doxo-induced senescent IMR-90s and in proliferative IMR-90s for all genes in the targeted custom sublibrary. R-squared value is from a linear regression model. Labelled in light green, gray, and dark green are hits passing 10% FDR only in the Doxo-induced senescent screen, only in the proliferative cell screen, or in both screens, respectively.

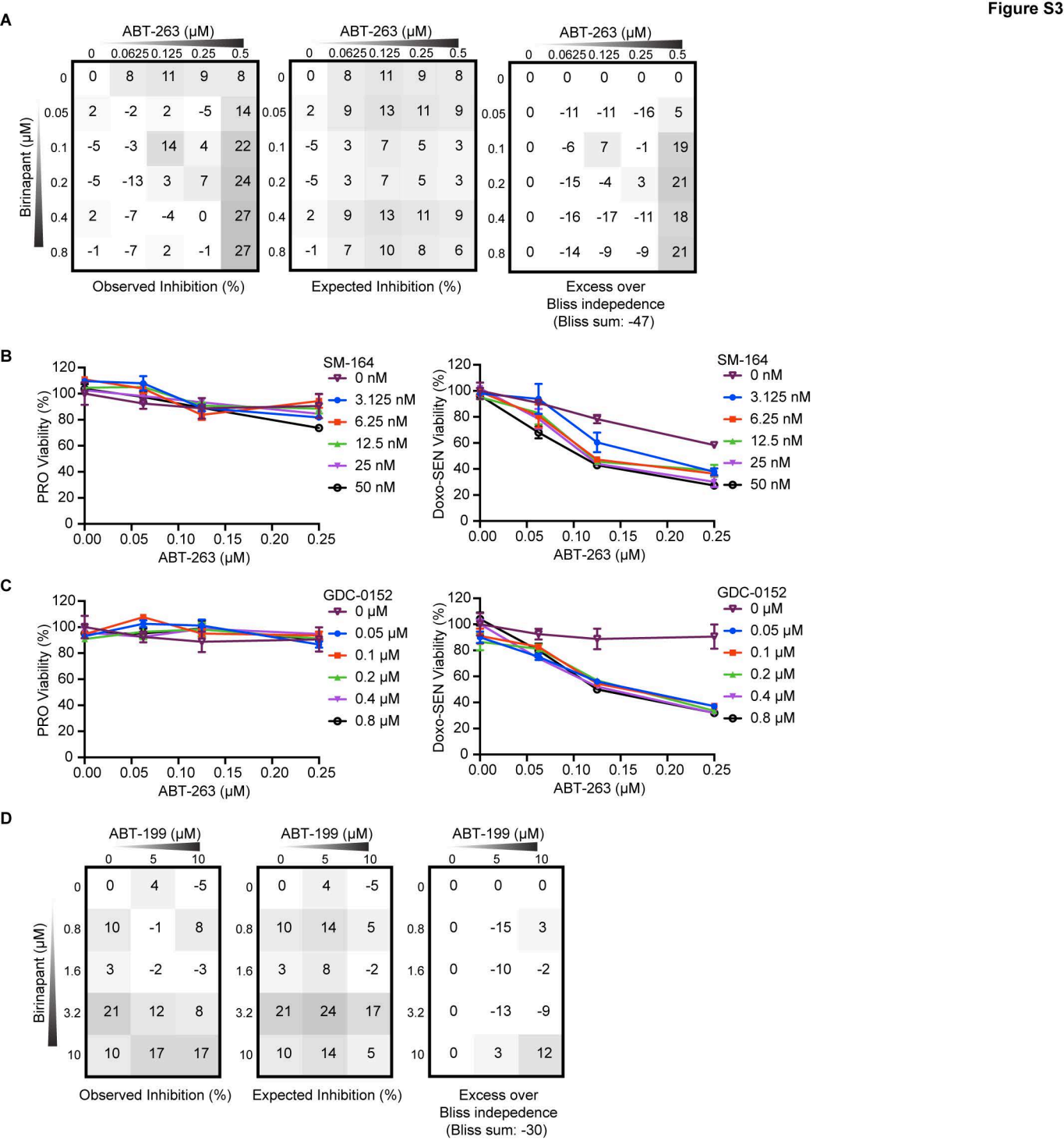
A
ABT-263 (μM)
0 0.0625 0.125 0.25 0.5
Birinapant (μM)
0 0 8 11 9 8
0.05 2 -2 2 -5 14
0.1 -5 -3 14 4 22
0.2 -5 -13 3 7 24
0.4 2 -7 -4 0 27
0.8 -1 -7 2 -1 27
Observed Inhibition (%)
0 0 8 11 9 8
0.05 2 9 13 11 9
0.1 -5 3 7 5 3
0.2 -5 3 7 5 3
0.4 2 9 13 11 9
0.8 -1 7 10 8 6
Expected Inhibition (%)
0 0 0 0 0 0
0.05 0 -11 -11 -16 5
0.1 0 -6 7 -1 19
0.2 0 -15 -4 3 21
0.4 0 -16 -17 -11 18
0.8 0 -14 -9 -9 21
Excess over
Bliss indepedence
(Bliss sum: -47)
B
PRO Viability (%)
ABT-263 (μM)
SM-164
0 nM
3.125 nM
6.25 nM
12.5 nM
25 nM
50 nM
Doxo-SEN Viability (%)
C
GDC-0152
0 μM
0.05 μM
0.1 μM
0.2 μM
0.4 μM
0.8 μM
D
ABT-199 (μM)
0 5 10
Birinapant (μM)
0 0 4 -5
0.8 10 -1 8
1.6 3 -2 -3
3.2 21 12 8
10 10 17 17
Observed Inhibition (%)
0 0 4 -5
0.8 10 14 5
1.6 3 8 -2
3.2 21 24 17
10 10 14 5
Expected Inhibition (%)
0 0 0
0.8 0 -15 3
1.6 0 -10 -2
3.2 0 -13 -9
10 0 3 12
Excess over
Bliss indepedence
(Bliss sum: -30)

Figure S3. SMAC mimetics synergize with ABT-263 and ABT-199 to induce death in senescent cells, related to Figure 4

(A) The percent expected inhibition is subtracted from the percent observed inhibition at each combination of drug doses in proliferative IMR-90s to calculate drug synergy represented by excess over Bliss independence. (B and C) Proliferative (left) and Doxo-induced senescent (right) IMR-90s were treated with ABT-263 and the indicated SMAC mimetic at the indicated concentrations for 3 d before viability was assessed relative to no drug control. (D) The percent expected inhibition is subtracted from the percent observed inhibition at each combination of drug doses in proliferative IMR-90s to calculate drug synergy represented by excess over Bliss independence. Data are representative of two independent experiments performed in triplicate and presented as mean ± s.e.m. in panels (A-D).

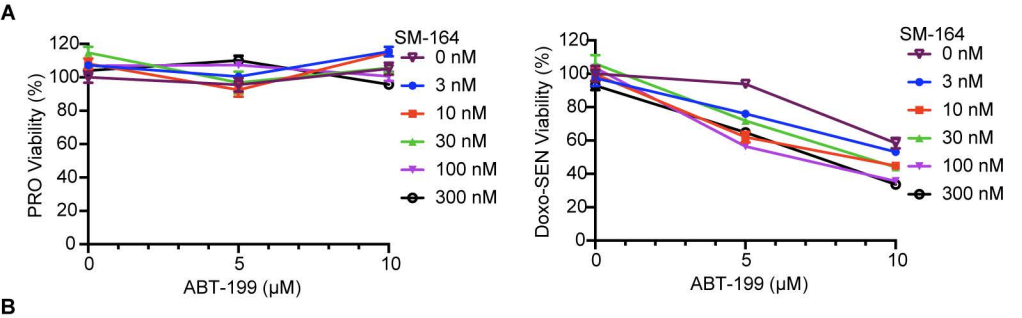
A
PRO Viability (%)
ABT-199 (μM)
SM-164
0 nM
3 nM
10 nM
30 nM
100 nM
300 nM
Doxo-SEN Viability (%)

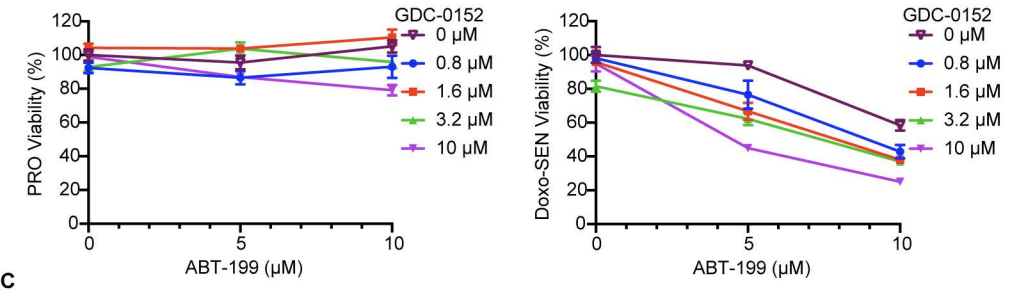
B
PRO Viability (%)
ABT-199 (μM)
GDC-0152
0 μM
0.8 μM
1.6 μM
3.2 μM
10 μM
Doxo-SEN Viability (%)

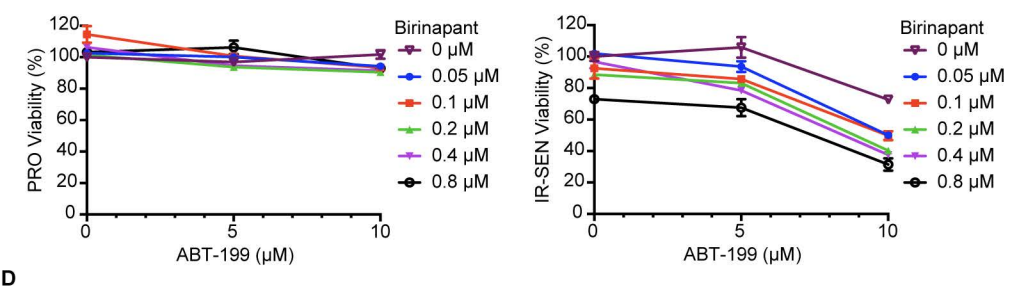
C
PRO Viability (%)
ABT-199 (μM)
Birinapant
0 μM
0.05 μM
0.1 μM
0.2 μM
0.4 μM
0.8 μM
IR-SEN Viability (%)

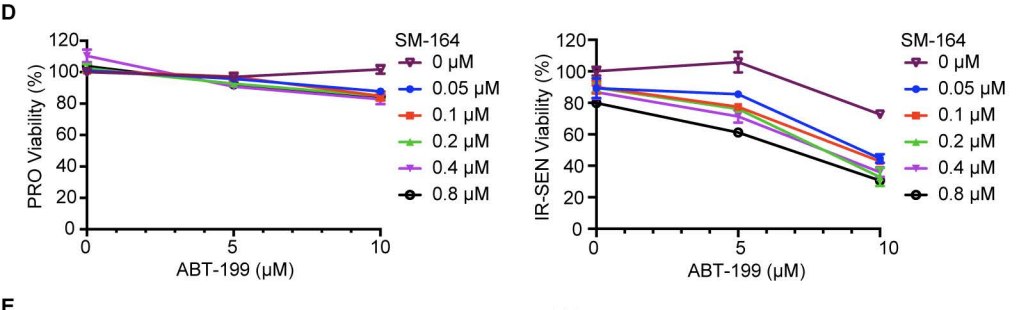
D
PRO Viability (%)
ABT-199 (μM)
SM-164
0 μM
0.05 μM
0.1 μM
0.2 μM
0.4 μM
0.8 μM
IR-SEN Viability (%)

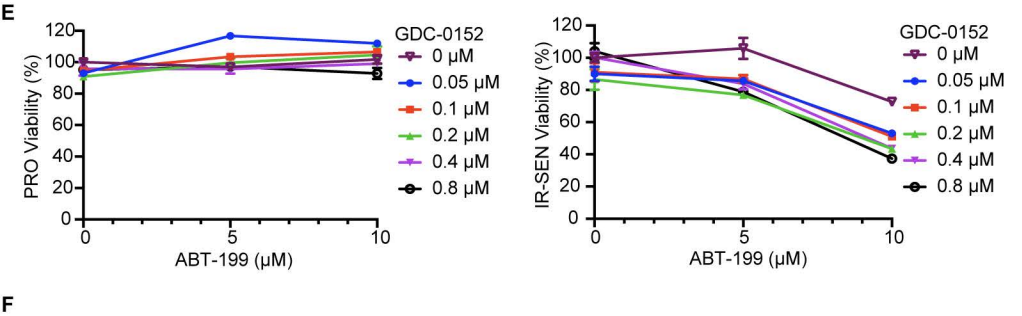
E
PRO Viability (%)
ABT-199 (μM)
GDC-0152
0 μM
0.05 μM
0.1 μM
0.2 μM
0.4 μM
0.8 μM
IR-SEN Viability (%)

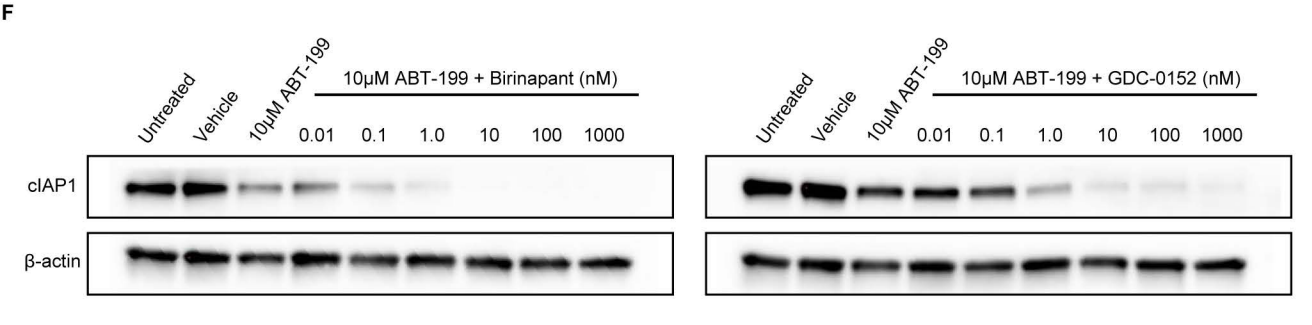
F
Untreated
Vehicle
10μM ABT-199
10μM ABT-199 + Birinapant (nM)
0.01
0.1
1.0
10
100
1000
10μM ABT-199 + GDC-0152 (nM)
cIAP1
β-actin

Figure S4. Multiple different SMAC mimetics synergize with ABT-199 to induce death in doxorubicin and irradiation-induced senescent cells, related to Figure 4

(A and B) Proliferative (left) and Doxo-induced senescent (right) IMR-90s were treated with ABT-199 and the indicated SMAC mimetic at the indicated concentrations for 3 d before viability was assessed relative to no drug control. (C-E) Proliferative (left) and IR-induced senescent (right) IMR-90s were treated with ABT-199 and the indicated SMAC mimetic at the indicated concentrations for 3 d before viability was assessed relative to no drug control. (F) Western blots of cIAP1 levels in IR-SEN IMR-90s treated with ABT-199 and varying doses of SMAC mimetic (either birinapant (left) or GDC-0152 (right)), to examine if inhibition is being achieved at doses which are synergistic for cell viability. Loading control, β-Actin. Data are representative of two independent experiments performed in triplicate and presented as mean ± s.e.m. in panels (A-E).

Figure S5

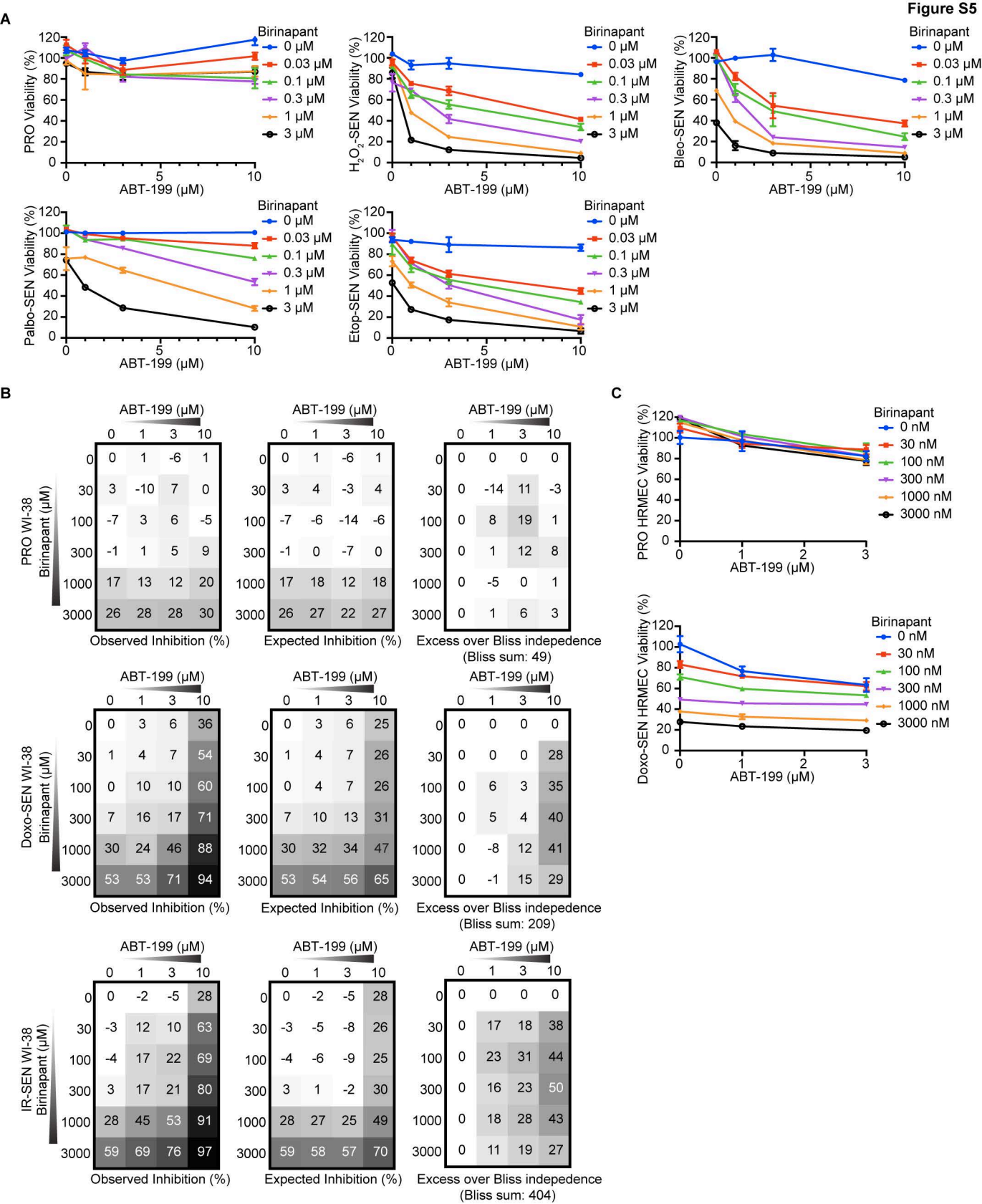
A
PRO Viability (%)
H2O2-SEN Viability (%)
Bleo-SEN Viability (%)
Palbo-SEN Viability (%)
Etop-SEN Viability (%)
ABT-199 (μM)
Birinapant
0 μM
0.03 μM
0.1 μM
0.3 μM
1 μM
3 μM
B
PRO WI-38
Doxo-SEN WI-38
IR-SEN WI-38
Birinapant (μM)
ABT-199 (μM)
Observed Inhibition (%)
Expected Inhibition (%)
Excess over Bliss indepedence
(Bliss sum: 49)
(Bliss sum: 209)
(Bliss sum: 404)
C
PRO HRMEC Viability (%)
Doxo-SEN HRMEC Viability (%)
ABT-199 (μM)
Birinapant
0 nM
30 nM
100 nM
300 nM
1000 nM
3000 nM

Figure S5. SMAC mimetics synergize with ABT-199 to induce selective senescent cell death across different senescence inducers and cell types, related to Figure 5

(A) Proliferative and senescent IMR-90s induced by treatment with hydrogen peroxide (H_2O_2), bleomycin (Bleo), palbociclib (Palbo), and etoposide (Etop) as indicated were treated with ABT-199 and birinapant at the indicated concentrations for 3 d before viability was assessed relative to no drug control. (B) The percent expected inhibition is subtracted from the percent observed inhibition at each combination of drug doses in proliferative (top), Doxo-induced senescent (middle), and IR-induced senescent (bottom) WI-38s to calculate drug synergy represented by excess over Bliss independence. (C) Proliferative (top) and Doxo-induced senescent (bottom) HRMECs were treated with ABT-199 and birinapant at the indicated concentrations for 3 d before viability was assessed relative to no drug control. Data are representative of two independent experiments performed in triplicate and are presented as mean ± s.e.m. in panels (A-C).

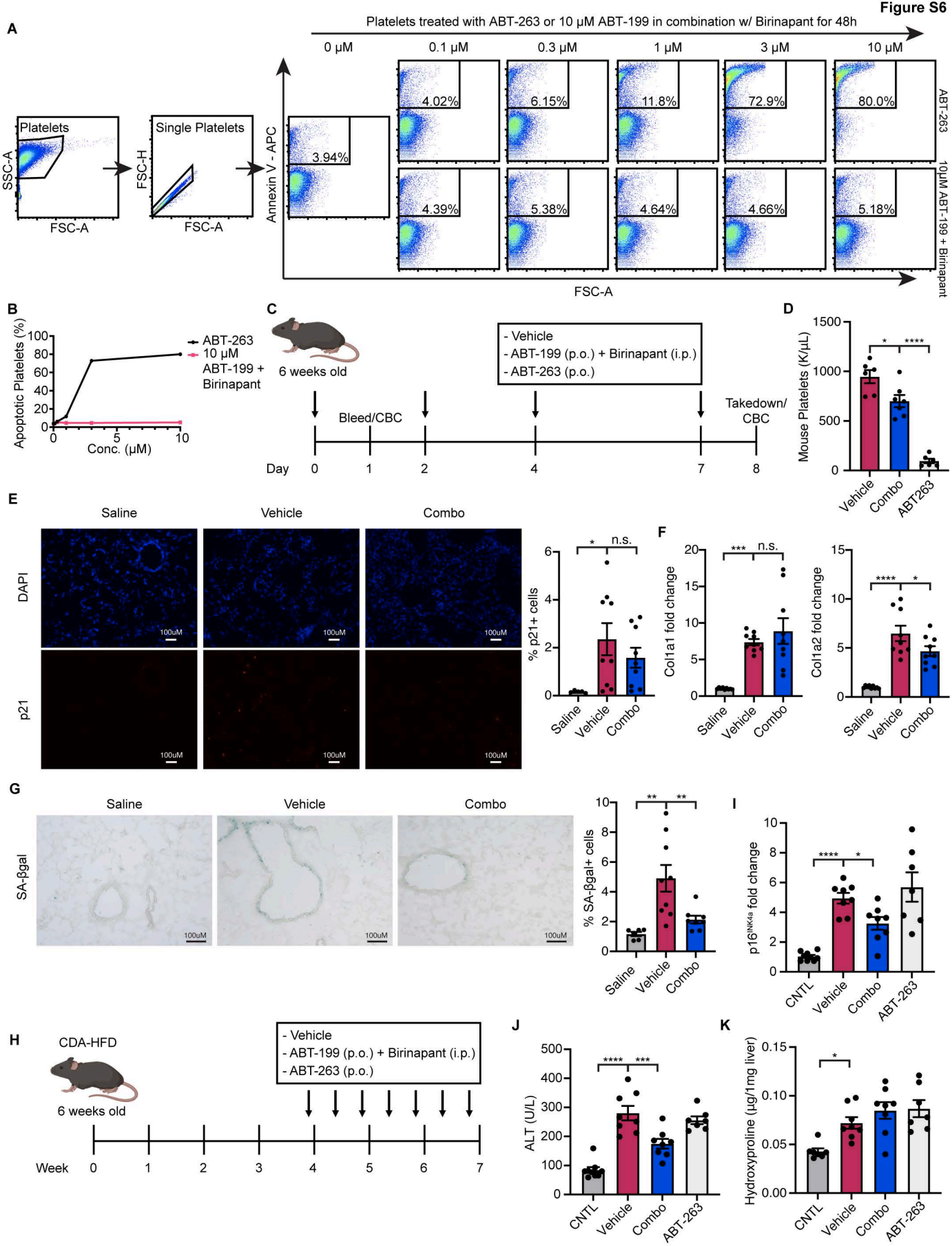
A
Platelets treated with ABT-263 or 10 μM ABT-199 in combination w/ Birinapant for 48h
0 μM
0.1 μM
0.3 μM
1 μM
3 μM
10 μM
Platelets
SSC-A
FSC-A
Single Platelets
FSC-H
FSC-A
Annexin V - APC
3.94%
4.02%
6.15%
11.8%
72.9%
80.0%
4.39%
5.38%
4.64%
4.66%
5.18%
ABT-263
10μM ABT-199 + Birinapant
FSC-A
B
Apoptotic Platelets (%)
Conc. (μM)
ABT-263
10 μM ABT-199 + Birinapant
C
6 weeks old
- Vehicle
- ABT-199 (p.o.) + Birinapant (i.p.)
- ABT-263 (p.o.)
Bleed/CBC
Takedown/ CBC
Day 0 1 2 4 7 8
D
Mouse Platelets (K/μL)
Vehicle
Combo
ABT263
E
Saline
Vehicle
Combo
DAPI
p21
100uM
% p21+ cells
n.s.
F
Col1a1 fold change
Col1a2 fold change
G
SA-βgal
% SA-βgal+ cells
I
p16INK4a fold change
CNTL
Vehicle
Combo
ABT-263
H
CDA-HFD
6 weeks old
- Vehicle
- ABT-199 (p.o.) + Birinapant (i.p.)
- ABT-263 (p.o.)
Week 0 1 2 3 4 5 6 7
J
ALT (U/L)
K
Hydroxyproline (μg/1mg liver)

Figure S6. ABT-199 and SMAC mimetic combination spares human platelets and reduces levels of senescent cell markers in vivo including in a model of NASH, related to Figure 6
(A) Representative flow cytometry plots of apoptosis in human platelets indicated by Annexin V staining after treatment with vehicle, the indicated doses of ABT-263, or the combination of 10 μM ABT-199 and the indicated doses of birinapant for 48 h. (B) Quantification of (A). (C) Schematic of in vivo mouse platelet toxicity experiment. (D) Platelet count from mice treated with vehicle, ABT-199 in combination with birinapant, or ABT-263, one day after initiation of treatment. (E) Representative images and quantification of DAPI (top) and p21 (bottom) stained lung sections from saline control (left), vehicle-treated (middle), and ABT-199/birinapant-treated (right) mice. Scale bar: 100 μm. (F) mRNA expression of *p21*, *Col1a1*, and *Col1a2* in murine lungs from the in vivo IPF experiment were quantified by qRT-PCR and normalized by Tbp levels. Fold-increase was calculated with respect to the mRNA levels in saline-treated control mice. (G) Representative images and quantification of SA-βgal stained lung sections (with a focus on the bronchioles area) from saline control (left), vehicle-treated (middle), and ABT-199/birinapant-treated (right) mice. Scale bar: 100 μm. (H) Schematic of NASH mouse model experiment. (I) mRNA expression of $p16^{INK4a}$ in murine livers were quantified by qRT-PCR and normalized by Tbp levels. Fold-increase was calculated with respect to the mRNA levels in control mice. (J) Serum alanine aminotransferase (ALT) levels were determined from NASH mice as treated in (H). (K) Collagen content of liver samples measured using hydroxyproline assays. For panel (D) n = 6 vehicle and ABT-263 group, n = 7 combo group. For panel (E), n = 5 in saline-treated controls and n = 9 in each of the vehicle-treated and ABT-199/birinapant-treated groups. For panel (F) n = 9 mice for each group. For panel (G) n = 6 saline control, n = 9 vehicle-treated, and and 8 ABT-199/birinapant-treated. For panels (I and J) n = 9 control group, n = 8 vehicle and combo groups, and n = 7 ABT-263 group. For panel (K) n = 7 control and ABT-263 groups, n = 8 vehicle and combo groups. One-way ANOVA with Dunnett's post-hoc test, *P < 0.05, **P < 0.01, ***P < 0.001, ****P < 0.0001.

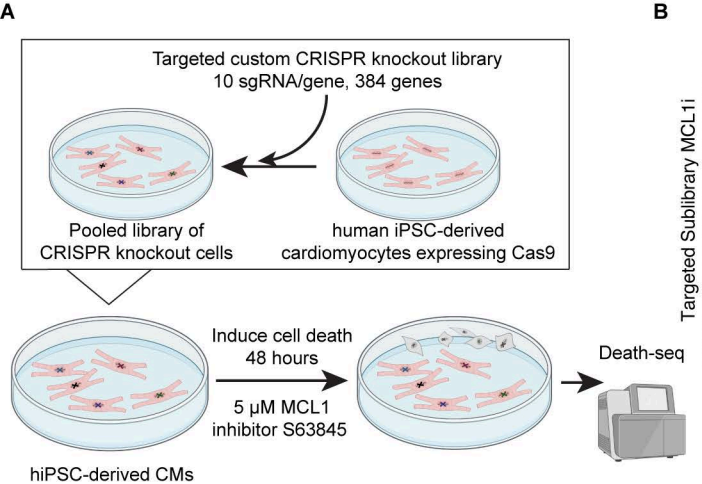
A
Targeted custom CRISPR knockout library
10 sgRNA/gene, 384 genes
Pooled library of
CRISPR knockout cells
human iPSC-derived
cardiomyocytes expressing Cas9
Induce cell death
48 hours
5 μM MCL1
inhibitor S63845
hiPSC-derived CMs
Death-seq

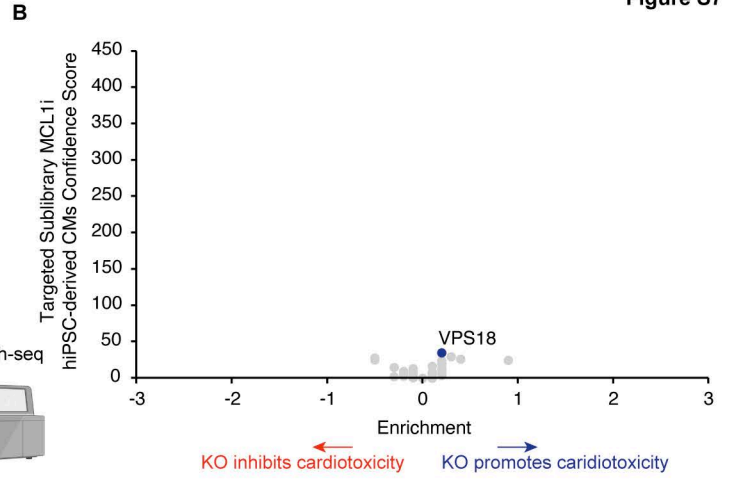
B
Targeted Sublibrary MCL1i
hiPSC-derived CMs Confidence Score
450
400
350
300
250
200
150
100
50
0
VPS18
-3
-2
-1
0
1
2
3
Enrichment
KO inhibits cardiotoxicity
KO promotes caridiotoxicity

Figure S7. Death-seq does not bias towards direct regulators of apoptosis in screen of cardiotoxicity for human iPSC-derived cardiomyocytes, related to Figure 7

(A) Schematic of Death-seq sublibrary CRISPR KO screens for modifiers of cardiotoxicity induced by 5 μM of the MCL1 inhibitor S63845 for 48 h in human iPSC-derived cardiomyocytes. (B) Volcano plot of the effects and confidence scores of all the genes in the sublibrary CRISPR screen for modifiers of cardiotoxicity induced by the MCL1 inhibitor S63845. Effects and casTLE scores are calculated by casTLE. Labelled are the genes passing 30% FDR for inhibiting (red) or promoting (blue) cell death when knocked out. See also the results and raw sequencing counts from screens in Tables S1 and S2 respectively.